https://doi.org/10.15255/KUI.2022.010
KUI-57/2022
Original scientific paper
Received February 12, 2022
Accepted July 31, 2022

# Drying Process of Cement Mortar Composites Reinforced with Cellulosic Fibres: Experiment and Mathematical Modelling

*A. Lachenani*,[a] *M. Bentchikou*,[b] *M. Boumahdi*,[a] *S. Hanini*,[a] and *M. Laidi*[a*]

[a] Laboratory of Biomaterials and Transport Phenomena (LBMPT), University of Médéa, Algeria
[b] Laboratory of Mechanics, Physics and Mathematical Modelling (LMP2M), University of Médéa, Algeria



**Abstract**

In this paper, six novel mathematical models based on semi-empirical calculus are proposed and applied to characterise the oven-drying process of cement mortar composites reinforced with cellulosic fibres (CMCRCFs). The drying experiments were carried out on four levels of oven-drying temperatures (70, 85, 105, and 120 °C), with four different cellulosic fibres content (0, 5, 10, and 20 %). Obtained results were compared to those derived by regression analysis of six most typically used mathematical drying models (Newton, Page, Page modified1, Page modified2, Handerson Pabis, and Logarithmic) in addition to six proposed models. The regression accuracy of the drying process was evaluated by the coefficient of determination ($R^2$), low mean square error (MSE), low root mean squared error (RMSE), and mean absolute error (MAE). Additional criteria were used to ensure more validity of the selected models. The obtained values indicate a highly accurate fit of the proposed model MR9, meaning that the proposed model can clearly interpret the experimental drying data and predict the dry state of CMCRCFs.

**Keywords**

*Cement mortar composites, cellulosic fibres, oven drying, modelling, regression analysis*

## 1 Introduction

Due to their good mechanical properties and low cost, cement-based materials, such as composite mortars and cement pastes are still widely used in building and road construction. In addition, interest has increased in the use of cellulosic fibres as alternatives for conventional reinforcements in composites. The development of commercially viable, environmentally friendly, and healthy materials based on natural resources is on the rise.[1] In this sense, cellulosic fibres as reinforcements for cement mortar composites constitute a very interesting option for the construction industry. Vegetable and cellulosic fibre cement composites exhibit improved toughness, ductility, flexural capacity, and crack resistance compared with non-fibre-reinforced cement-based materials.[2–4] The significant advantage of fibre reinforcement is the behaviour of the composite after cracking has started, as the fibres bridge the matrix cracks and transfer the loads. The post-cracking toughness allows more extensive use of such composites in construction. Such extensive use of mortar cement is due to its good mechanical properties, low cost, but also its durability, which is one of the important parameters.[1] The water-retaining properties of cementitious materials are an essential indicator of their durability. However, the water flow through the mortar pores can also indicate greater ease of degradation.[5] The study of the interaction between water and solid, in particular during the drying process, is one of the keys for durability studies of cement products.

Drying of porous materials is a complex process of simultaneous heat and mass transfer characterised by external convective heat and mass transfer to the drying medium, and internal transport within the wet solid. The complex interaction between the solid, the different mechanisms of heat and mass transfer, lead to difficulties in the explication of the internal transport of the drying process. Furthermore, the mechanism of moisture migration is dominated by many physical variables at different drying stages, and the transport coefficients are a function of moisture content and temperature within the porous body during the drying operation. The drying process occurs mainly in two stages: The first phase is characterised by linear weight loss over time. During this step, the speed at which moisture reaches the material surface is faster than the rate at which moisture is evaporated. The surface where evaporation takes place is the drying front. In the second phase, moisture transport slows down and the vapour content lost to the environment is higher than the content that actually reaches the surface. At this stage, the drying front is inside the material and no longer on its surface, so the vapour diffusion from the interior to the surface of the material is increased.[5]

Drying process of cement-based porous materials is required to investigate their microstructure, strength, and drying characteristics. Moreover, clarifying the kinetics of drying is desirable for optimising the drying process, which is significant for engineering, managing waste to obtain ecological material, and developing new drying devices.[6]

Concrete drying appears to be a well-known process due to years of experimental investigation. However, concrete drying is a complicated process that is influenced by a wide range of factors, including concrete composition, age, environmental factors, and local temperature and humidity in a concrete member.[7]

* Corresponding author: Maamar Laidi, PhD
Email: maamarw@yahoo.fr; laidi.maamar@univ-medea.dz

In most industrial drying operations, heat is supplied externally to a product by a drying medium to provide energy for moisture evaporation and removal. Numerous drying techniques to remove water from dense porous solids have been developed, such as oven-drying, perchlorate-drying, spray-drying, vacuum-drying, dry-ice-drying, freeze-drying, methanol–pentane exchange-drying, and pulse-spouted microwave-drying,[8–11] but oven-drying remains the most commonly used and probably the cheapest drying method to remove water confined in cement-based porous materials (CBPMs). Water removal from porous solids can be governed by moisture diffusion, capillary flow, and sorption-based mechanisms, which generate various drying models.[11]

However, due to the complexity of drying kinetic, which is affected greatly by temperature and mass transfer process, two categories of theoretical drying models exist. The first one is the sorption-based mechanisms, which are based on Fick's second law of diffusion, because the transport process of water from porous solids is generally considered to be dominated by molecular water diffusion. The second one is the diffusion-based mechanisms where the transport process of moisture from a porous material is generally considered to be dominated by moisture diffusion.[8] Numerous solutions and approximations of this equation are proposed leading to easily having the moisture profile inside the material and its variation with time.[12]

Drying process is well represented by the drying curve that gives information about the variation of the moisture ratio with time under several experimental conditions. According to previous studies done for porous materials such as cement mortar,[12] and some building materials;[13] air temperature**,** relative air humidity, and its velocity are found as the most influential parameters.

In the current study, the air velocity was kept constant, and the effect of temperature and cellulosic fibre content on cement mortar composites reinforced with cellulosic fibres (CMCRCFs) were investigated.

This paper aims to present experimental measurements of the drying of CMCRCFs specimens to compare results with predictions acquired by numerical modelling of the moisture diffusion process.

Firstly, an oven-drying series of tests were carried out on CMCRCFs specimens under various temperatures, specifically: 70, 85, 105, and 120 °C in order to model the drying phenomena. Furthermore, six novel mathematical models were developed to characterise the drying process of CMCRCFs and optimise drying control conditions.

## 2 Materials and methods

### 2.1 Materials

The cellulosic fibres used in this study were obtained by recycling eggs packaging. Portland cement, type CPJ-CEM II/A 42.5 N, from (Djelfa cement company, Algeria) was used for preparing mortar composites. The sand used was a mixture of natural sand and crushing sand with a fineness modulus of 2.5. Proportions of natural sand and crushing sand were 51.75 and 48.25 %, respectively. Tap water was used for the mortar preparation. For all mixtures, the rate of mixing water was variable due to the use of cellulosic fibres.

In this work, four cellulosic fibre weight fractions of cement were designed to study the influence of the CF content on drying kinetics. For each test, three duplicates were used for the drying tests at the designated age. In total, forty-eight samples were cast in 40 mm × 40 mm × 160 mm moulds.

The mixed proportions of studied mortars and their notations are presented in Table 1.

*Table 1* – Composition of materials and mass proportions

| Description | $m_{(cement)}$ / g | $m_{(water)}$ / g | $m_{(sand)}$ / g | $m_{(cellulosic\ fibres)}$ / g | W/C / – |
|---|---|---|---|---|---|
| CMC1 | 450.00 | 225.00 | 1350.00 | 0.00 | 0.50 |
| CMC2 | 379.77 | 311.41 | 1139.33 | 19.02 | 0.82 |
| CMC3 | 310.85 | 373.06 | 932.57 | 31.10 | 1.20 |
| CMC4 | 225.70 | 491.90 | 677.00 | 45.14 | 2.18 |

The proportion of cement and sand was kept constant (1 : 3). The reference sample (CMC1) was prepared according to the standard with W/C = 0.5 and without adding cellulosic fibres. For samples CMC2, CMC3, and CMC4, the amount of CF was added in portion of 5, 10, and 20 % from weight of cement, respectively. Cement to water ratio (W/C) was varied due to the changing amount of fibres used in the mixture, and considering the hydrophilic nature of CF. These constituents influence significantly the workability of mortars; as a result, the porosity and mechanical properties are also influenced.

All mixtures were prepared under the same conditions in a laboratory at a temperature of 20 ± 2 °C, and relative humidity greater than or equal to 50 %. The confection of the mixture was carried out according to European standard EN 196-1. Twenty-four hours later, samples were removed from the moulds and stored in a water container at 20 ± 2 °C until testing.

### 2.2 Drying process

To establish a drying kinetics model, the drying test was conducted for four groups of CMCRCFs (0, 5, 10, and 20 %) at four levels of temperature (70, 85, 105, and 120 °C).

Following the curing period of 28 days in water, the specimens were removed from the tank. They were wiped with a wet cloth, and wrapped with two layers of plastic film for 48 h to ensure uniform distribution of water in specimens. Each sample of each mixture was then weighed and equally spaced in the oven, which was preheated to a specific temperature for the drying test.

A ventilated and temperature-programming oven was used for the drying test. The weight loss measurement during the experiments was performed by a balance with a sensitivity level of 0.001 g.

The drying test was conducted as follows: firstly, the dryer was preheated at the desired temperature. The humid specimens were weighed and placed on a stainless-steel sieve. The set was introduced into the oven. The water loss ($m_t$–$m_d$) and time ($t$) of drying were recorded during the drying test.

The drying procedure was stopped once the relative mass loss was less than or equal to 0.05 %. The last recorded weight loss ($m_0$-$m_d$) was used for calculating the moisture ratio, where: $m_0$, $m_t$, and $m_d$ are the mass of the specimen before drying, during drying, and after drying, respectively. For each material, three independent tests were carried out to verify the reproducibility and reliability of the experiments.

## 3 Mathematical modelling

In this work, we focus on the characterisation of the drying process of CMCRCFs using various models describing moisture transport in concrete, which can be found in the literature. These models are empirical, physical, or a combination of both. Some of them are mentioned further. The experimental drying data were accommodated to twelve drying models (six models from the literature and six models proposed in this study), given in Table 2, using MATLAB software version 2008.

The purpose was to determine the moisture content as a function of drying time. The selected models were applied to evaluate the model that best described the oven-drying behaviour of CMCRCFs during the drying process, where $k$, $k_1$, $k_2$, $a$, $b$, $\alpha$, $\beta$, and $\gamma$ are constants of the models, and $t$ is time (h). The dimensionless moisture ratio $MR$ and the drying rate $DR$ are given by:

$$MR = \frac{m_t - m_d}{m_0 - m_d} \tag{1}$$

$$DR = \frac{m_{t+\Delta t} - m_t}{\Delta t} \tag{2}$$

The non-linear regression analysis was used by means of a non-linear least square method of the scaled Levenberg–Marquardt algorithm. Twelve drying models (6 from the literature and 6 proposed) were investigated. The appropriate model for the description of the drying kinetics of CMCRCFs samples was chosen according to the following criteria: The highest coefficient of determination ($R^2$) and low root mean squared error (RMSE).[14–16] The best-performing model was selected based on the smallest average error (RMSE ≈ 0) and the largest coefficient of determination ($R^2$ ≈ 1), which were used as indicators of goodness of fit.

The main purpose of mathematical modelling is prediction. To ensure greater reliability and accuracy of the regression analysis, diverse statistical quantities were used; mean square error (MSE), mean absolute error (MAE), root mean square error (RMSE), and coefficient of determination ($R^2$), which are given by the following formulas:[17–19]

*Table 2* – Drying models

| *Description* | *Model* | *Expression* |
|---|---|---|
| MR1 | Lewis | $MR = e^{-k t}$ |
| MR2 | Henderson | $MR = a\,e^{-k t}$ |
| MR3 | Logarithmic | $MR = a\,e^{-k t} + b$ |
| MR4 | Page | $MR = e^{-k t^{\alpha}}$ |
| MR5 | Page 1 | $MR = a\,e^{-k t^{\alpha}}$ |
| MR6 | Page 2 | $MR = a\,e^{-k t^{\alpha}} + b$ |
| MR7 | Proposed Model 1 | $MR = e^{-k_1 t^{\alpha} - k_2 t^{\beta}}$ |
| MR8 | Proposed Model 2 | $MR = a\,e^{-k_1 t^{\alpha}} - (1-b)\,e^{-k_2 t^{\beta}}$ |
| MR9 | Proposed Model 3 | $MR = \frac{1 - a t^{\alpha} e^{-k_1 t^{\alpha}}}{1 - b t^{\alpha} e^{-k_2 t^{\alpha}}}$ |
| MR10 | Proposed Model 4 | $MR = a + b\,e^{-k_1 t} + d\,e^{-k_2 t^{\beta}}$ |
| MR11 | Proposed Model 5 | $MR = \left(e^{-(k_1 t^{\alpha} + k_2 t^{\beta})}\right)^{\gamma}$ |
| MR12 | Proposed Model 6 | $MR = a\left(e^{-(k_1 t^{\alpha} + k_2 t^{\beta})}\right)^{\gamma}$ |

$$R^2 = 1 - \frac{\sum_{i=1}^{N}\left(MR_i^{\text{cal}} - MR_i^{\text{exp}}\right)^2}{\sum_{i=1}^{N}\left(MR_i^{\text{cal}} - \overline{MR}_i^{\text{exp}}\right)^2} \tag{3}$$

$$\text{RMSE} = \sqrt{\frac{1}{N}\sum_{i=1}^{N}\left(MR_i^{\text{exp}} - MR_i^{\text{cal}}\right)^2} \tag{4}$$

$$\text{MSE} = -\sum\left(MR_i^{\text{exp}} - MR_i^{\text{cal}}\right) \tag{5}$$

$$\text{MAE} = \frac{1}{N}\sum_{i=1}^{N}\left|MR_i^{\text{exp}} - MR_i^{\text{cal}}\right| \tag{6}$$

where $i$ is the $i^{\text{th}}$ drying test, and $N$ is the total number of measurements for each drying test. The closer the values of RMSE, MSE, and MAE are to zero, and the closer the $R$-square is to 1, the more accurate the model results will be.

The following criteria were used to ensure more validity of the selected model. These statistics are given as follows:[17]

Acceptability criterion, *K* factor,

$$K = \frac{\sum_{i=1}^{N} MR_i^{\text{exp}} MR_i^{\text{cal}}}{\sum_{i=1}^{N} \left(MR_i^{\text{cal}}\right)^2} \tag{7}$$

Acceptability criterion, *K′* factor,

$$K' = \frac{\sum_{i=1}^{N} MR_i^{\text{exp}} MR_i^{\text{cal}}}{\sum_{i=1}^{N} \left(MR_i^{\text{exp}}\right)^2} \tag{8}$$

where $0.85 \leq K \leq 1.15$ and $0.85 \leq K' \leq 1.15$ are acceptability criteria.[17]

$$R_0^2 = 1 - \frac{\sum_{i=1}^{N} \left(MR_i^{\text{cal}} - K\, MR_i^{\text{cal}}\right)^2}{\sum_{i=1}^{N} \left(MR_i^{\text{cal}} - \overline{MR}_i^{\text{cal}}\right)^2} \tag{9}$$

$$R_1^2 = 1 - \frac{\sum_{i=1}^{N} \left(MR_i^{\text{exp}} - K\, MR_i^{\text{exp}}\right)^2}{\sum_{i=1}^{N} \left(MR_i^{\text{exp}} - \overline{MR}_i^{\text{exp}}\right)^2} \tag{10}$$

$$R_{\text{m}}^2 = R^2 \left(1 - \sqrt{\left|R^2 - R_0^2\right|}\right) \tag{11}$$

where $R_{\text{m}}^2 \geq 0.5$ is acceptability criterion.[17]

$$MF = \frac{R^2 - R_0^2}{R^2} \tag{12}$$

$$NF = \frac{R^2 - R_1^2}{R^2} \tag{13}$$

where $MF \leq 0.1$ and $NF \leq 0.1$ are acceptability criteria.[17]

## 4 Results and discussion

A representative comparison of drying profiles at different temperatures for different cellulosic fibres content is shown in Fig. 1.

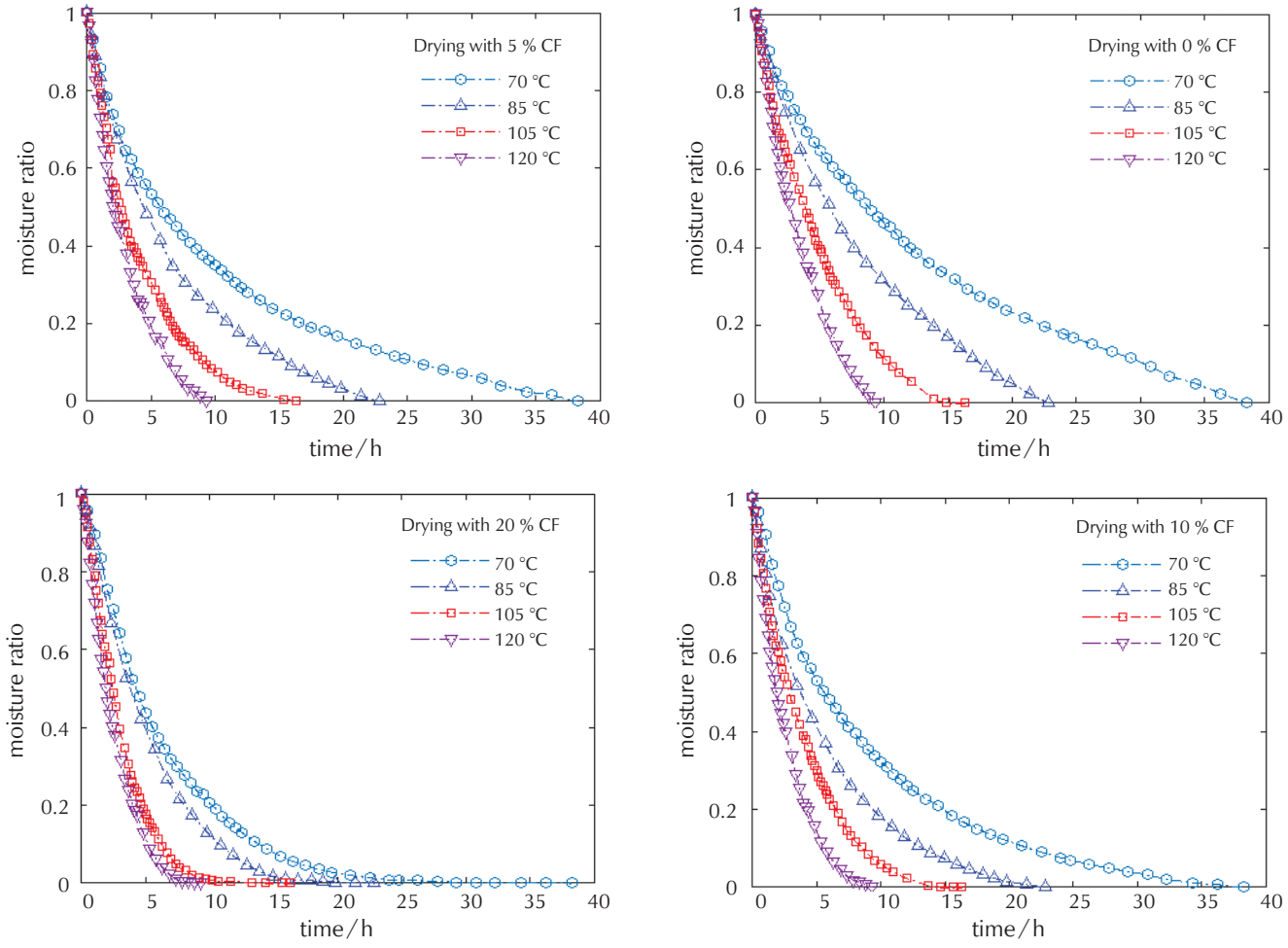


*Fig. 1* – Effect of temperature and cellulosic fibres content on the drying kinetics

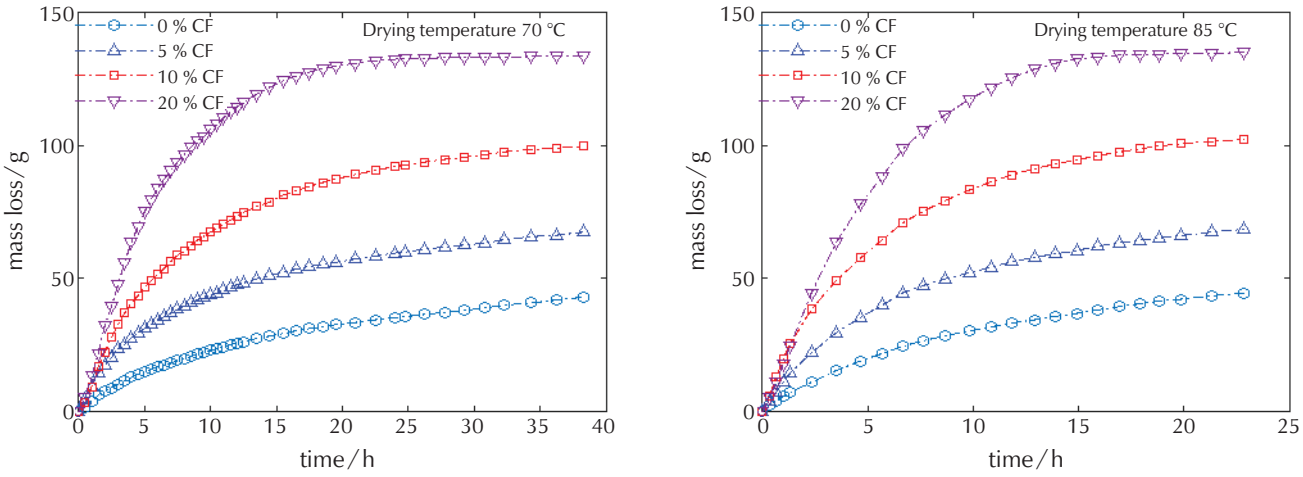


*Fig. 2* – Mass loss at $T = 70$ °C and $T = 85$ °C with drying time

### 4.1 Effect of drying temperature

As may be seen from the curves, by increasing air temperature, the drying process is accelerated due to an increase in evaporation rate. In addition, at constant air temperature, increasing the cellulosic fibres content accelerates the drying process due to a high heat transfer potential.

The effects of different drying temperatures on concrete strength were studied by [20], who found that a drying temperature above 85 °C is reasonable and efficient for drying tests of standard concrete cube specimens.

For cement-based porous material, performing oven-drying at 105 °C is very efficient for removing water. However, such a high temperature can also remove the structural water of hydration products and lead to decomposition of the ettringite phase.[8] Therefore, using a moderate drying temperature (60 °C or lower) could be a better way to obtain drying efficiency while maintaining the microstructure of cement-based porous material.[8]

### 4.2 Effect of cellulosic fibres content on the drying kinetics

During drying, the effect of cellulosic fibres content is significant where the high fibres content samples have more void space and present more moisture, thus, it has a longer constant rate period. This can be explained by the fact that, at low porosity, it is difficult to pump out the moisture by capillary forces for a longer time, while at high porosity, the free moisture content is higher, which allows the capillary forces to keep the surface wet above critical moisture content for a longer time.[13] At falling rate period, higher fibre content samples have a higher drying rate, because the moisture diffusion and movement are easier and diffuse faster to the sample surface. This is shown in Fig. 1 where the highly porous sample dried faster than the other samples.[7]

In addition, a significant and rapid water mass loss was observed in the early drying period for all the samples. Fig. 2 shows that more than 50 % of the confined water was removed from the pores of CMCRCFs, after the first 5 h of drying for all samples at a drying temperature of 70 °C and 85 °C. The mass-loss rates decreased but remained rapid as drying time proceeded. The drying profiles show a knee point around (10 h), before and after which the mass loss curves are significantly different. This can be explained by the fact that water -an important component of CMCRCFs, has a low density but occupies remarkable volumes; it is thus reasonable that samples with a higher W/C ratio show greater water loss during drying,[11] as may be seen in Fig. 2 for the CMCRCFs with 20 % fibre content.

It is evident from Fig. 3 that the drying rate of CMCRCFs samples reached the maximum value rapidly and then gradually decreased.

The maximum drying rate was observed for the higher cellulosic fibres content specimens. It was also noticed that drying temperatures and cellulosic fibres content greatly influence the general drying rate curve trend of the CMCRCFs. The drying rate curves indicate that the drying process of the specimens can be divided into two stages, namely speedup and speed-down,[20] except in the cases of 0 % of cellulosic fibres content at 70 °C and 85 °C, which shows only a falling-rate drying period. As the drying temperature increases, the drying process of the CMCRCFs becomes fast and significant water is lost.[20]

### 4.3 Modelling of drying kinetics

To study the drying kinetics, the models listed in Table 2 were fitted to the measured data with adjustable parameters. To simplify the comparison, the performances of each model are shown in Table 3 and Fig. 4.

Table 3 shows the statistical performances of 12 mathematical models based on the most commonly used criteria, such as ($R^2$, MAE, and RMSE), and the acceptability criteria ($K$, $K'$, $MF$ and $NF$). It is noticeable that data fitting results are consistent with all of the criteria.

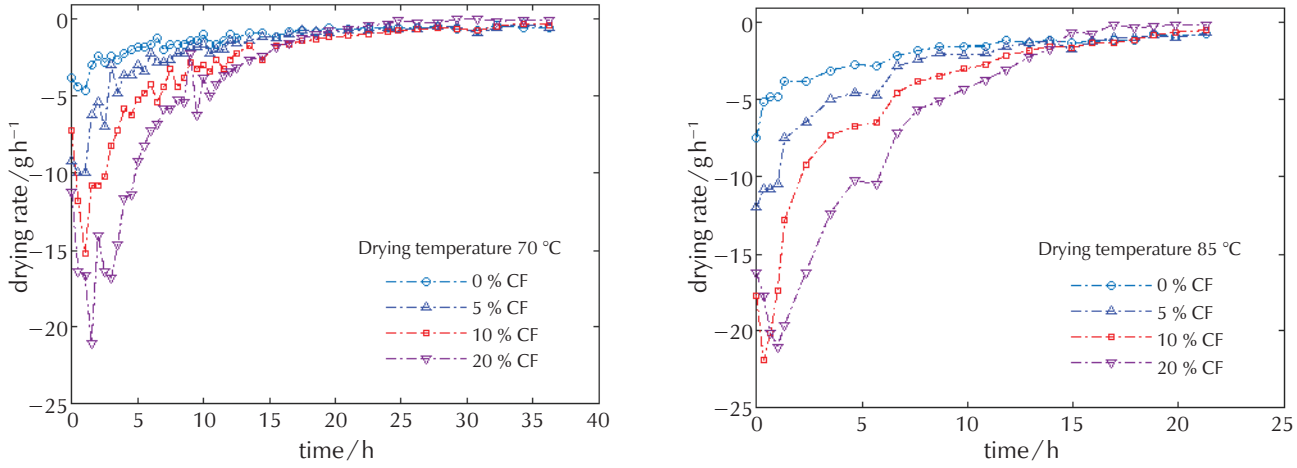


*Fig. 3* – Drying rate at $T = 70$ °C and $T = 85$ °C

The comparison between the performances of the different models indicates that the model proposed in this work, MR9, provides the best correlation performance, where the value of $\overline{\text{RMSE}}$ is (≈ 0.52 %). The second-best correlation performance is given by the proposed model MR8, where the $\overline{\text{RMSE}}$ has a value of (≈ 0.62 %).

The results in Fig. 4 show that all the fitting curves captured the experimental data with good or advanced agreement, with determination coefficients close to 1 ($R^2 > 0.9900$). This suggests that the analytical models in Table 2 can describe the drying kinetics of CMCRCFs.

### 4.4 Evaluation of the best-fit models

The first comparison between the models MR6, MR7, MR8, MR9, MR10, MR11, and MR12 is presented in the form of kinetics curves in which the moisture ratio (*MR*) is plotted for the entire database.

The variation of the predicted moisture ratio with the experimental moisture ratio is shown in Fig. 4 for the CMCRCFs with 5 % cellulosic fibre content at 70, 85, 105, and 120 °C.

The comparison of the models results showed that the equation of the models MR6, MR7, MR8, MR9, MR10, MR11, and MR12 fitted the best by taking into account

*Table 3* – Statistical quantities for tested models

| *Description* | *Model* | $R^2$ | $K$ | $K'$ | $R^2_0$ | $R^2_1$ | $R^2_m$ | RMSE | MSE | MAE | *MF* | *NF* |
|---|---|---|---|---|---|---|---|---|---|---|---|---|
| MR1 | Lewis | 0.9932 | 1,0055 | 0.9929 | 0.9986 | 0.9987 | 0.9237 | 0.0231 | 0.0006 | 0.0190 | −0.0110 | −0.0111 |
| MR2 | Henderson | 0.9957 | 1.0000 | 0.9984 | 1.0000 | 1.0000 | 0.9325 | 0.0189 | 0.0004 | 0.0150 | −0.0088 | −0.0088 |
| MR3 | Logarithmic | 0.9977 | 1.0000 | 0.9991 | 1.0000 | 1.0000 | 0.9526 | 0.0134 | 0.0002 | 0.0109 | −0.0046 | −0.0046 |
| MR4 | Page | 0.9976 | 0.9990 | 0.9985 | 1.0000 | 1.0000 | 0.9518 | 0.0135 | 0.0002 | 0.0109 | −0.0047 | −0.0047 |
| MR5 | Page modified 1 | 0.9978 | 1.0000 | 0.9992 | 1.0000 | 1.0000 | 0.9532 | 0.0132 | 0.0002 | 0.0023 | −0.0044 | −0.0044 |
| MR6 | Page modified 2 | 0.9992 | 1.0000 | 0.9997 | 1.0000 | 1.0000 | 0.9714 | 0.0082 | 0.0001 | 0.0064 | −0.0017 | −0.0017 |
| MR7 | Proposed Model 1 | 0.9985 | 1.0012 | 0.9983 | 1.0000 | 1.0000 | 0.9633 | 0.0104 | 0.0001 | 0.0082 | −0.0029 | −0.0029 |
| MR8 | Proposed Model 2 | 0.9995 | 1.0000 | 0.9998 | 1.0000 | 1.0000 | 0.9783 | 0.0062 | 0.0000 | 0.0048 | −0.0011 | −0.0011 |
| MR9 | Proposed Model 3 | 0.9996 | 0.9998 | 1.0000 | 1.0000 | 1.0000 | 0.9818 | 0.0052 | 0.0000 | 0.0041 | −0.0007 | −0.0008 |
| MR10 | Proposed Model 4 | 0.9991 | 0.9998 | 0.9999 | 1.0000 | 1.0000 | 0.9724 | 0.0079 | 0.0001 | 0.0055 | −0.0018 | −0.0018 |
| MR11 | Proposed Model 5 | 0.9983 | 1.0020 | 0.9974 | 1.0000 | 1.0000 | 0.9610 | 0.0111 | 0.0001 | 0.0086 | −0.0033 | −0.0033 |
| MR12 | Proposed Model 6 | 0.9989 | 1.0000 | 0.9996 | 1.0000 | 1.0000 | 0.9677 | 0.0092 | 0.0001 | 0.0073 | −0.0022 | −0.0022 |

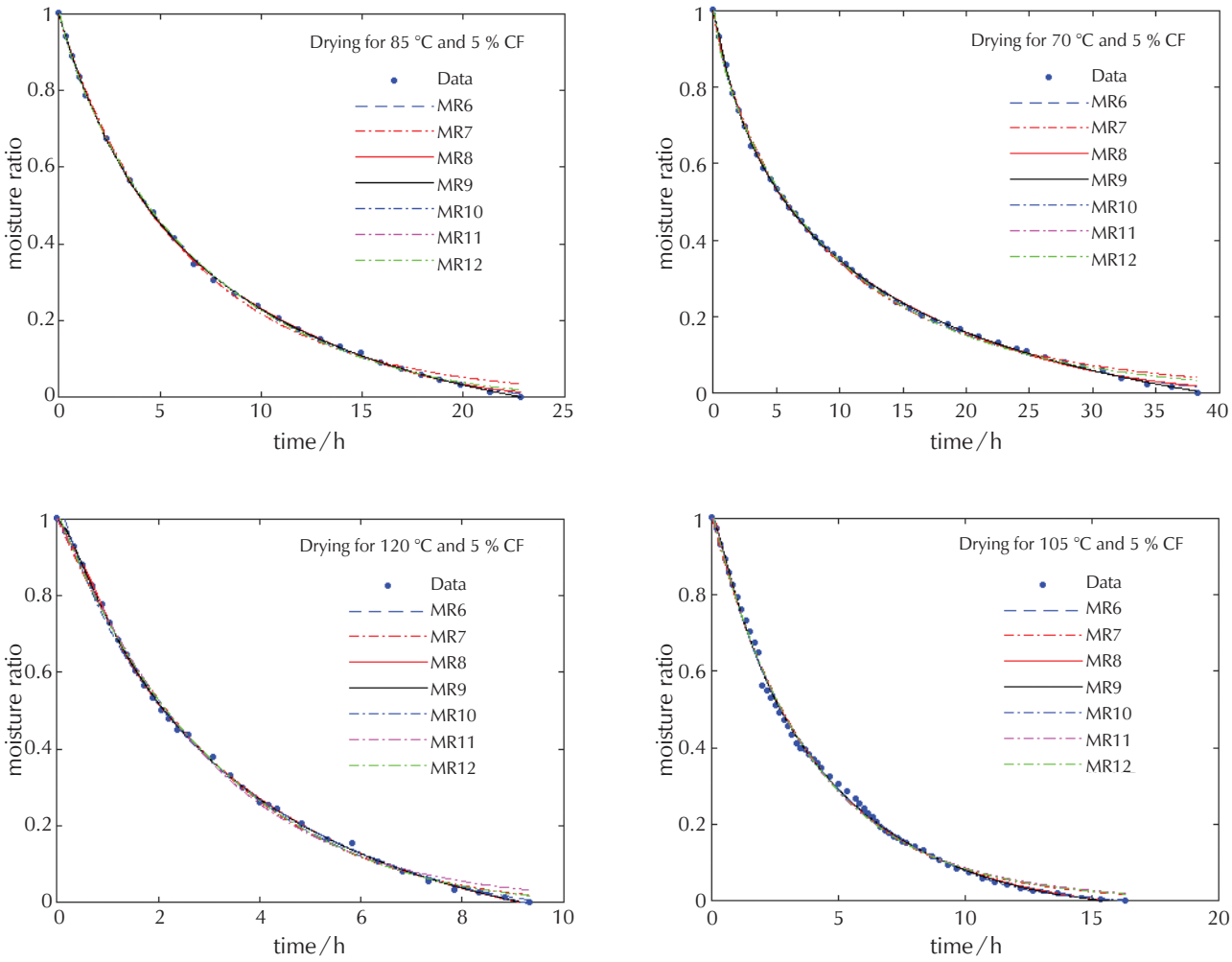


*Fig. 4* – Calculated data from proposed models *vs* experiment data

the coefficient of determination $R^2$, the constants $K$, $K'$, $MF$, and $NF$.

The correlation coefficient ($R^2$), mean absolute error (MAE), and two constants $K$ and $K'$ are shown in Table 3. The new MR9 model had the highest value of $R^2$ and the lowest value of MAE.

The absolute mean error was found 0.41, 0.48, 0.64, and 0.55 % for the MR9, MR8, MR6, and MR10 models, respectively. The new MR9 model had the lowest value of MAE, so it was chosen as the more suitable with the experimental data.

The second comparison was made in terms of linear regression between the predicted and experimental moisture ratio to assess the ability of the proposed MR9 model to describe the oven-drying kinetics. Fig. 5 shows the juxtaposition of the first bisector and the line of the best linear fit of the calculated with the experimental values of moisture ratio. The distribution of the experimental points confirms excellent agreement between the moisture ratio calculated by the best proposed MR9 model and that of the experiment at 70 °C for various fibre content, and at different temperatures for 5 % of fibre content.

### 4.5 Comparison with previous results

For comparison purposes, the drying curves were plotted. They were characterised by the graphical representation of the evolution of the moisture ratio (generally a decrease in the moisture ratio). In addition, the drying kinetics is represented by drying rate *versus* drying time.

Previous research works have shown that the drying curves of cement-based porous material have the same general trend.[11,12,20] However, a significant difference had been observed in total drying time and mass loss due to the different applied drying conditions such as samples shape and size, composition, water to cement ratio, drying temperature, relative humidity, and air velocity around the material.

Furthermore, introducing fibres in mortar composition greatly influences the drying kinetics, where the drying time decreases and the drying rate varies significantly at different drying temperatures. Table 4 describes the applied conditions of some drying tests.

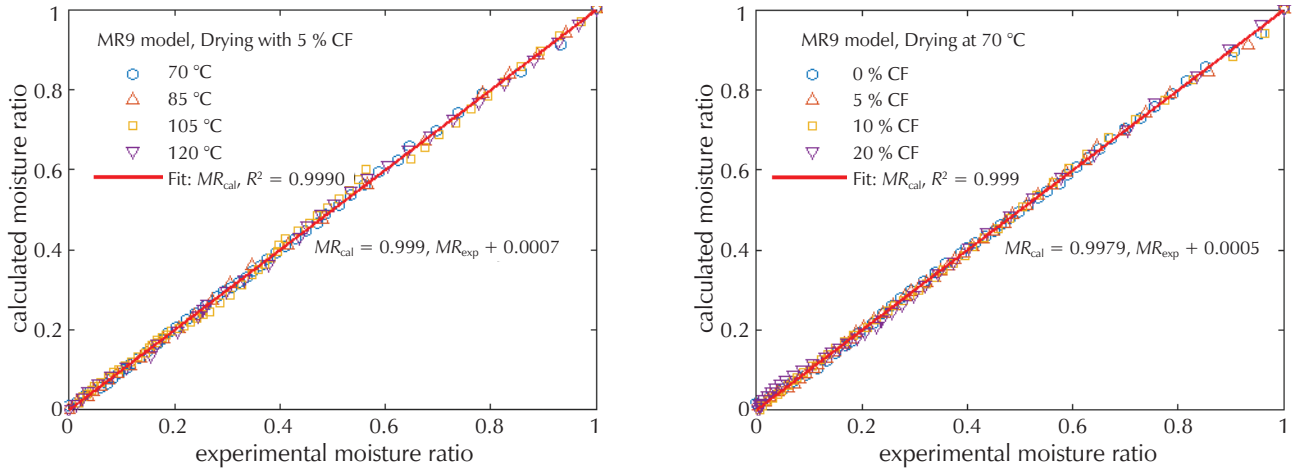


*Fig. 5* – Calculated *vs* experimental moisture ratio using MR9 model

*Table 4* – Description of drying test conditions for comparison

| Authors | Samples | W/C | Shape | Curing condition | Size | Drying temperature / °C |
|---|---|---|---|---|---|---|
| *Bennamoun et al.*[12] | cement mortar | 0.5 | cylindrical shape | in water | diameter = 13 mm<br>height = 17 mm | 60, 90, 130 |
| *Zhang et al.*[20] | concrete | 0.55 | cube | in water | length = 150 mm | 60, 85, 105, 120, 150 |
| in this study | cement mortar reinforced with cellulosic fibres | 0.5 | parallelepiped shape | in water | width = 40 mm<br>depth = 40 mm<br>length = 160 mm | 70, 85, 105, 120 |

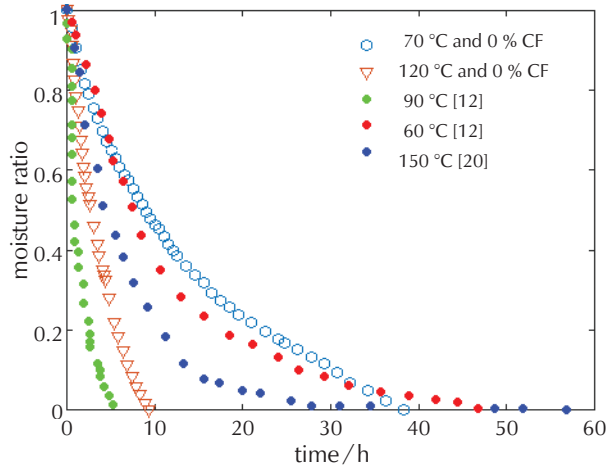


*Fig. 6* – Drying curves for comparison

Fig. 6 brings together the drying curves from this study and other references at different temperature levels. All the curves have the same general trend. However, a difference in the shape of individual curves is observed. This difference is due to the following factors: The shape and size of specimens (cylinder, cube, and parallelepiped), and the material (cement mortar, concrete, and cement mortar reinforced with cellulosic fibres). Reviewing these factors can be very useful in identifying the changes that can be seen over time in a drying process.

## 5 Conclusion

In this paper, a set of experiments to characterise the oven-drying process of cement mortar composites reinforced with cellulosic fibres was performed. The results obtained allow us to conclude that:

- The drying curves have a similar trend regardless of the CF content.
- The CF content has an important influence on the drying time of CMCRCFs. The required drying time for CMCRCFs decreases by about 50 % with the temperature rising from 70 to 105 °C. In addition, CMCRCFs samples with higher cement content have lower mass loss compared to those with higher CF content.
- The different drying kinetics of samples could be explained by their different pore structures due to different W/C ratios.
- Increasing temperature and cellulosic fibre content is an efficient way to augment the drying rates of CMCRCFs.
- The drying rate curves show that the drying process occurs in two stages for samples with 0 % cellulosic fibre content, and in three stages for samples with 5, 10, and 20 % cellulosic fibre content.
- Most of the models used in this study were found to be able to capture the drying profiles of CMCRCFs, but the proposed new MR9 model provides excellent accuracy. This model can describe the drying kinetics of CM-

CRCFs for parallelepiped specimens at temperatures extending from 70 to 120 °C.

- The results suggest that further experimentation and investigation should be carried out to confirm the validity of the proposed models.

ACKNOWLEDGEMENTS

We thank the General Direction of Scientific Research and Technological Development (DGRSDT) and the Laboratory of Biomaterials and Transport Phenomena (LBMPT) of the University of Médéa for funding this work.

## List of abbreviations and symbols

C – cement, g

CF – cellulosic fibres

CMC – composition of cement mortar composite

CMCRCFs – cement mortar composites reinforced with cellulosic fibres

$DR$ – drying rate, g h$^{-1}$

$K$, $K'$ – acceptability criterion, –

$\overline{K}$, $\overline{K'}$ – average value of the accessibility criterion, –

$k$, $k_1$, $k_2$, $a$, $b$, $\alpha$, $\beta$, $\gamma$ – constants of the models

MAE – mean absolute error, –

$\overline{\text{MAE}}$ – average value of the mean absolute errors, –

$MR$ – moisture ratio, –

$MR^{\text{cal}}$ – calculated moisture ratio, –

$MR^{\text{exp}}$ – experimental moisture ratio, –

$\overline{MR}$ – average value of the moisture ratio, –

$MF$ – $M$ factor, –

$\overline{MF}$ – average value of the $M$ factors, –

MSE – mean square error, –

$\overline{\text{MSE}}$ – average value of the mean square error, –

$NF$ – $N$ factor, –

$\overline{NF}$ – average value of the $N$ factors, –

$R^2$ – coefficient of determination, –

$\overline{R^2}$ – average value of $R^2$, –

RMSE – root mean squared error, –

$\overline{\text{RMSE}}$ – average value of root mean squared errors, –

$T$ – drying temperature, °C

$t$ – drying time recorded during the drying test, h

W – water, g

## References
## Literatura

1. *M. Ardanuy, J. Claramunt, R. D. Toledo Filho,* Cellulosic fiber reinforced cement-based composites: A review of recent research, Constr. Build. Mater. **79** (2015) 115–128, doi: https://doi.org/10.1016/j.conbuildmat.2015.01.035.
2. *H. Savastano Jr, P. G. Warden, R. S. P. Coutts,* Mechanically pulped sisal as reinforcement in cementitious matrices, Cem. Concr. Compos. **25** (3) (2003) 311–319, doi: https://doi.org/10.1016/S0958-9465(02)00055-0.
3. *J. H. Morton, T. Cooke, S. A. S. Akers,* Performance of slash pine fibers in fiber cement products, Constr. Build. Mater. **24** (2010) 165–170, doi: https://doi.org/10.1016/j.conbuildmat.2007.08.015.
4. *R. D. Toledo Filho, K. Ghavami, G. L. England,* Development of vegetable fibre-mortar composites of improved durability, Cem. Concr. Compos. **25** (2003) 185–196, doi: https://doi.org/10.1016/S0958-9465(02)00018-5.
5. *M. C. F. Salomão, E. Bauer, C. S. Kazmierczak*, Drying parameters of rendering mortars, Ambiente Construído **18** (2018) 7–19, doi: https://doi.org/10.1590/s1678-86212018000200239.
6. *Q Li, S Xu, Q Zeng,* A fractional kinetic model for drying of cement-based porous materials, Dry. Technol. **34** (10) (2016) 1231–1242, doi: https://doi.org/10.1080/07373937.2015.1103255.
7. *M. Vinkler, J. L. Vítek,* Drying concrete: experimental and numerical modeling, J. Mater. Civil Eng. **28** (9) (2016) 04016070, doi: https://doi.org/10.1061/(ASCE)MT.1943-5533.0001577.
8. *K. K. Aligizaki,* Pore Structure of Cement-Based Materials: Testing, Interpretation and Requirements, Taylor & Francis, London and New York, 2006.
9. *N. C. Collier, J. H. Sharp, N. B. Milestone, J. Hill,* The influence of water removal techniques on the composition and microstructure of hardened cement pastes, Cem. Concr. Res. **38** (6) (2008) 737–744, doi: https://doi.org/10.1016/j.cemconres.2008.02.012.
10. *Q. Zeng, K. Li, T. Fen-Chong, P. Dangla,* Water removal by freeze-drying of hardened cement paste, Dry. Technol. **31** (1) (2013) 67–71, doi: https://doi.org/10.1080/07373937.2012.717326.
11. *Q. Zhang, Q. Zeng, DC. Zheng, J. Wang*, Oven dying kinetics and status of cement-based porous materials for in-lab microstructure investigation, Adv. Cement Res. **30** (5) (2018) 204–215, doi: https://doi.org/10.1680/jadcr.17.00075.
12. *L. Bennamoun, L. Kahlerras, F. Michel*, Determination of moisture diffusivity during drying of mortar cement: experimental and modelling study, Int. J. Energy Eng. **3** (2013) 1–6, url: http://hdl.handle.net/2268/140569.
13. *M. Karoglou, A. Moropoulou, Z. B. Maroulis,* Drying kinetics of some building materials, Dry. Technol. **23** (1-2) (2005) 305–315, doi: https://doi.org/10.1081/DRT-200047926.
14. *A. Mahdad, M. Laidi, S. Hanini, M. Hentabli*, Modelling the Drying Kinetics of Apple (Golab Variety): Fractional Calculus *vs* Semi-empirical Models, Kem. Ind. **70** (5-6) (2021) 251–262, doi: https://doi.org/10.15255/KUI.2020.051.
15. *O. Badaoui, S. Hanini, A. Djebli, B. Haddad, A. Benhamou,* Experimental and modelling study of tomato pomace waste drying in a new solar greenhouse: Evaluation of new drying models, Renew. Energy **133** (2019) 144–155, doi: https://doi.org/10.1016/j.renene.2018.10.020.
16. *S. Keskes, S. Hanini, M. Hentabli, M. Laidi*, Artificial Intelligence and Mathematical Modelling of the Drying Kinetics of Pharmaceutical Powders, Kem. Ind. **69** (3-4) (2020) 137–152, doi: https://doi.org/10.15255/KUI.2019.038.
17. *A. Benyekhlef, B. Mohammedi, S. Hanini, M. Boumahdi, A. Rezrazi, M. Laidi,* A, Contribution to the Modelling of Fouling Resistance in Heat Exchanger-Condenser by Direct and Inverse Artificial Neural Network, Kem. Ind. **70** (11-12) (2021) 639–650, doi: https://doi.org/10.15255/KUI.2020.076.

18. *R. Soleimani, A. H. S. Dehaghani, N. A. Shoushtari,* Toward an intelligent approach for predicting surface tension of binary mixtures containing ionic liquids, Korean J. Chem. Eng. **35** (7) (2018) 1556–1569, doi: https://doi.org/10.1007/s11814-017-0326-4.
19. *A. Golbraikh, A. Tropsha*, Beware of q2!, J. Mol. Graph. Model. **20** (2002) 269–276, doi: https://doi.org/10.1016/S1093-3263(01)00123-1.
20. *L. Zhang, Q. Ren, Z. Li, G. Zhang*, Predicting the Drying of Concrete by an Anomalous Diffusion Model, J. Mater. Civil Eng. **31** (3) (2019) 04019010, doi: https://doi.org/10.1061/(ASCE)MT.1943-5533.0002620.

## SAŽETAK

### Proces sušenja kompozita cementne žbuke ojačane celuloznim vlaknima: eksperiment i matematičko modeliranje

*Amina Lachenani*,[a] *Mohamed Bentchikou*,[b] *Mouloud Boumahdi*,[a] *Salah Hanini*[a] i *Maamar Laidi*[a*]

U ovom radu predloženo je i primijenjeno šest novih matematičkih modela temeljenih na poluempirijskom proračunu za karakterizaciju procesa sušenja u pećnici kompozita cementne žbuke ojačane celuloznim vlaknima (CMCRCF). Pokusi sušenja provedeni su pri četiri razine temperature sušenja u pećnici (70, 85, 105 i 120 °C) s četiri različita udjela celuloznih vlakana (0, 5, 10 i 20 %). Dobiveni rezultati uspoređeni su s onima dobivenim regresijskom analizom šest najčešće primjenjivanih matematičkih modela sušenja (Newton, Page, Page modified1, Page modified2, Handerson Pabis i Logarithmic) uz šest predloženih modela. Regresijska točnost procesa sušenja procijenjena je koeficijentom determinacije ($R^2$), srednjom kvadratnom pogreškom (MSE), korijenom srednje kvadratne pogreške (RMSE) i srednjom apsolutnom pogreškom (MAE). Primijenjeni su i dodatni kriteriji da bi se osigurala veća valjanost odabranih modela. Dobivene vrijednosti pokazuju dobro slaganje predloženog modela MR9 s eksperimentalnim vrijednostima, što znači da predloženi model može jasno interpretirati eksperimentalne podatke o sušenju i predvidjeti suho stanje CMCRCF-a.

Ključne riječi
*Kompoziti cementne žbuke, celulozna vlakna, sušenje, modeliranje, regresijska analiza*

[a] *Laboratory of Biomaterials and Transport Phenomena (LBMPT), University of Médéa, Alžir*
[b] *Laboratory of Mechanics, Physics and Mathematical Modelling (LMP2M), University of Médéa, Alžir*

Izvorni znanstveni rad
*Prispjelo 12. veljače 2022.*
*Prihvaćeno 31. srpnja 2022.*